New
Contaminants

https://doi.org/10.48130/newcontam-0026-0021

Original Research

Open Access

Oxidant-dependent carbamazepine transformation: how aged microplastics modulate degradation pathways in UV-AOPs

Yuhui Wang, Xiaochao Zhou, Zhenyang Xu, Hang Liu, Xiaohui Wang* and Tingting Zhang*

Received: 11 May 2026

Revised: 15 July 2026

Accepted: 20 August 2026

Published online: 9 September 2026

Abstract

Microplastics (MPs) and pharmaceuticals, as emerging contaminants, are ubiquitous in wastewater, yet their interfacial interactions during UV-based advanced oxidation processes (UV-AOPs) in wastewater treatment plants (WWTPs) remain poorly understood. To address this knowledge gap, we selected polyamide (PA) as a representative MP and investigated its effects on the degradation of carbamazepine (CBZ) in three UV-AOP systems: UV/PMS, UV/H_2O_2, and UV/Cl. We found that aged PA MPs developed various environmentally persistent free radicals on their surfaces, which significantly enhanced the production of ·OH and $^1O_2$, thereby promoting CBZ degradation, with observed rate constants increased by 1.2 to 1.8 times. Degradation pathways involving oxidation, hydroxylation, and ring cleavage reactions were proposed, with system-dependent intermediates such as TPs 208, 151, and 241 identified. Toxicity and molecular structure analyses revealed that removal of the –$CONH_2$ group, hydroxyl substitution, and unsaturated ring formation may increase product toxicity. Furthermore, NO_3^- promoted CBZ degradation, HCO_3^- and humic acid inhibited it, while Cl^- effects were concentration- and system-dependent. This study provides a theoretical basis for elucidating the environmental behaviors of MPs and pharmaceuticals during wastewater treatment in WWTPs.

Keywords: Aged MPs, EPFRs, UV-AOPs, Transformation pathways, Reactive species

Highlights

- Aged MPs developed various environmentally persistent free radicals on their surfaces.
- Aged MPs increased the k_{obs} of CBZ degradation by 1.2 to 1.8 times.
- EPFRs significantly enhanced the yield of reactive species in the UV-AOP systems.
- CBZ transformation in different systems involved hydroxylation and ring-condensation.
- Hydroxyl substitution and unsaturated ring formation may enhance toxicity.

* Correspondence: Xiaohui Wang (wangxh@mail.buct.edu.cn); Tingting Zhang (zhangtt@mail.buct.edu.cn)
Full list of author information is available at the end of the article.

https://doi.org/10.48130/newcontam-0026-0021

Graphical abstract

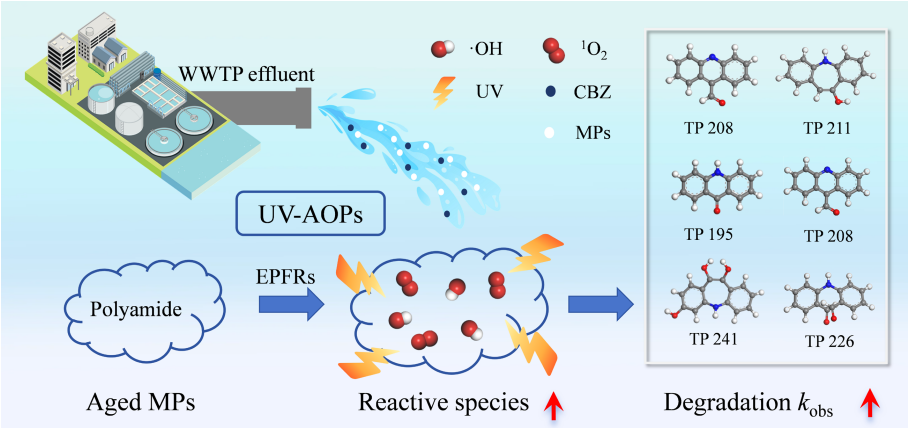

Introduction

Pharmaceuticals and personal care products (PPCPs) play a key role in the daily life of humans, and more than 4,000 kinds of PPCPs are currently used by humans and animal agriculture[1]. The parent compounds and most of the intermediates of PPCPs are eliminated from the body through biological metabolism. However, they cannot be effectively removed by sewage treatment plants, and they all end up in surface water, with concentrations ranging from ng·L^{-1} to μg·L^{-1}. Among them, carbamazepine (CBZ) is a pharmaceutical widely used for the treatment of epilepsy and neuropathic pain, with an annual global consumption of more than 1,000 tons[2]. In addition, CBZ has been frequently detected in surface water, wastewater, and drinking water[3], indicating its widespread occurrence in aquatic environments and potential ecological risks.

Since the 1940s, plastics have been widely applied across various fields globally[4]. The extensive use of plastics has led to serious environmental pollution, with particles smaller than 5 mm being defined as 'microplastics (MPs)'. Although the average concentration in open water bodies is relatively low, microplastics usually accumulate in wastewater treatment plants (WWTPs) and leachates from landfill sites. For instance, studies have documented microplastic concentrations reaching 1.3×10^5 and 10,044 particles·L^{-1} in the influent of WWTPs[5,6]. Due to characteristics such as small particle size and high specific surface area, MPs easily adsorb foreign pollutants, leading to the coexistence of MPs and pollutants in the aquatic environment, which affects the transport and transformation of pollutants[7,8]. Studies have reported that polyamide (PA) MPs are one of the most common polymers in WWTPs, primarily originating from textiles and synthetic clothing in daily life[9]. However, the ecological risks of PA have not been evaluated to the same extent as those of other MPs, such as polystyrene and polyethylene[10]. Therefore, it is urgent to explore the environmental behavior of PA in aquatic environments.

As both a source and sink of various organic pollutants, WWTPs serve as a critical stage before the entry of PPCPs into natural water bodies. Ultraviolet (UV) radiation activates oxidant precursors to generate reactive species that degrade PPCPs effectively. This mechanism confers UV-based advanced oxidation processes (UV-AOPs) numerous advantages such as chemical-free pathogen disinfection, simple maintenance, and low secondary pollution potential. In recent years, UV-AOPs have been extensively researched and applied in WWTPs[11,12]. For example, UV/PMS, UV/H_2O_2, and UV/Cl processes have been widely studied for the removal of various pollutants[13–15]. During the UV-AOPs process in WWTPs, MPs undergo physical abrasion, chemical oxidation, and other processes that alter their morphology and chemical characteristics, a phenomenon known as the aging of MPs. Previous studies suggest that MPs exhibit contradictory and complex effects on pollutant degradation; for instance, Sun et al. found that polyethylene promoted tetracycline degradation[16], and similarly, aged polystyrene was reported to facilitate the phototransformation of atorvastatin via enhanced reactive oxygen species generation[17]. Conversely, Wang et al. observed that polystyrene hindered cephalexin degradation[18], while other studies noted that coexisting MPs could alter transformation pathways and inhibit the formation of certain toxic intermediates during the degradation of fluorinated pollutants[19]. However, compared with pristine plastics, aged MPs exhibit more complex chemical properties (e.g., the formation of new C–Cl bonds and environmental persistent free radicals [EPFRs])[20], and their specific impacts on the transformation pathways and toxicity evolution of co-existing PPCPs remain largely unknown. Therefore, it is urgent to investigate the dual impact of aged MPs on the generation of reactive species and the environmental behavior of target pollutants (e.g., CBZ) during UV-AOP treatments. This study specifically focuses on alterations in molecular structure, degradation product abundance, and the resulting toxicity evolution, thereby providing a theoretical basis for elucidating the environmental behaviors of MPs and PPCPs in WWTPs.

Set against the research context of WWTPs, this study investigated the interfacial mechanisms between aged microplastics and CBZ in UV-AOPs, including UV/PMS, UV/H_2O_2, and UV/Cl systems, using PA as a typical MP. We also investigated the degradation kinetics of CBZ in different systems and the effect of aged MPs on CBZ degradation. A combination of experimental and characterization tools was used to identify the main active species affecting CBZ degradation in different systems, as well as the effect of aged MPs on the active species. In addition, we identified the major degradation intermediates of CBZ in different systems, proposed the degradation pathways of CBZ, and elucidated the effect of aged MPs on CBZ degradation. The toxicity of the intermediates was analyzed in relation to molecular structure and degradation product abundance. Finally, the effects of various environmental factors were examined. This study provided a theoretical basis for elucidating the environmental behaviors of MPs and PPCPs during the treatment of wastewater in WWTPs.

Materials and methods

Chemicals and reagents

All chemicals were of analytical grade, and all solutions were prepared using ultra-pure water. The details of chemicals are shown in Supplementary Text S1.

Experimental setup

The photochemical reaction device (CEL-LB70) used in this work was purchased from Beijing Zhongjiao Jinyuan Science and Technology Co. Ltd. The center of the setup contained the light source and was equipped with a magnetic stirring device and an efficient condensing reflux device. Six identical quartz reaction containers with a volume of 100 mL were evenly distributed around the light source. The UV light source was a 500 W high-pressure mercury lamp with a wavelength range of 200–400 nm and a light intensity of 25 mW·cm^{-2} measured with a UV radiometer.

Experimental methods

Aging treatment of MPs followed the method commonly adopted in the literature[19]. Detailed information is provided in Supplementary Text S2.

Experiments on the effect of aged MPs on the degradation performance of CBZ: 1 mg·L^{-1} of CBZ was added to each quartz tube, except for the control group where no MPs were added, and the rest of the quartz tubes were supplemented with 2 g·L^{-1} of the MPs. This MP concentration was selected as a model experimental condition to ensure a measurable and reproducible effect of aged MPs on CBZ degradation and to facilitate mechanistic investigation. The experiments were conducted in a photochemical reactor with a condensation sleeve and a 500 W mercury lamp as the UV light source. Samples were taken at 0, 0.25, 0.5, 1, 1.5, and 2 h. After sampling, each sample was filtered with a 0.22 μm filter membrane, quenched with a saturated sodium thiosulfate solution, and immediately analyzed by high-performance liquid chromatography (HPLC). All experiments were performed in triplicate. Dark adsorption and environmental factor experiments are shown in Supplementary Text S3.

ROS quenching experiments were carried out in quartz tubes by spiking with 40 mM of different quenching agents. The degradation kinetics of CBZ were fitted using a pseudo-first-order kinetic model: $\ln(C_0/C_t) = k_{obs}t$, where C_0 and C_t are the concentrations of CBZ at time 0 and t, respectively, and k_{obs} is the reaction rate constant. Tert-butanol (TBA), furfuryl alcohol (FFA), *p*-benzoquinone (*p*-BQ), and benzoic acid (BA) were used to scavenge ·OH, $^1O_2$, $O_2^{\cdot-}$, and Cl·, respectively. The other parameters remained the same as in the degradation performance experiments.

Analytical methods

The concentration of CBZ was determined using HPLC (Essentia SPD-16, Shimadzu, Japan) with a UV detector at 286 nm. The column temperature was 25 °C, and the injection volume was 20 μL. The mobile phase was selected as 1‰ formic acid/acetonitrile (5/5 v/v), and the flow rate was 1.0 mL·min^{-1}. The analysis time for each sample was 3.25 min. Degradation intermediates of CBZ were analyzed by ultra-performance liquid chromatography (Waters, Milford, MA, USA) with a triple quadrupole time-of-flight mass spectrometer (XEVO G2 QTOF, Waters Micromass, Manchester, UK). Electron paramagnetic resonance (EPR, Bruker E500) spectroscopy was employed to detect the presence of free radicals and nonradical species. The toxicity of CBZ and its degradation intermediates was assessed with the Ecological Structure Activity Relationship (ECOSAR) procedure. Toxicity was classified into four classes (very toxic, toxic, harmful, and not harmful) according to the Globally Harmonised System of Classification and Labelling of Chemicals[21].

Results and discussions

Degradation kinetics of CBZ in UV/AOP/aged MPs system

We investigated the degradation properties of CBZ in UV/PMS, UV/H_2O_2, and UV/Cl systems, and examined the effects of different concentrations of oxidants (0, 0.05, 0.1, 0.2, 0.5, and 1.0 mM) on CBZ degradation. As shown in Supplementary Figs. S1–S3, the degradation processes of CBZ in UV-AOPs followed pseudo-first-order kinetics. In the UV/PMS system, the kinetic constant for CBZ degradation increased from 0.37 to 3.01 h^{-1} with increasing PMS concentration. At a PMS concentration of 0.2 mM, the k_{obs} of CBZ reached 1.98 h^{-1}. For the UV/H_2O_2 and the UV/Cl systems, the k_{obs} increased from 0.18 and 0.08 to 0.74 and 0.73 h^{-1} with increasing oxidant concentration, respectively. Considering the actual oxidant concentrations used in wastewater treatment plants, findings from previous studies, and the degradation rates of CBZ observed in this study, a concentration of 0.2 mM was selected for subsequent oxidant additions[22,23]. We further investigated the effect of aged MPs on CBZ degradation with PA, as shown in Fig. 1 and Supplementary Figs. S4–S6. In the UV/PMS-aged MPs system, the k_{obs} of CBZ degradation was 2.30 h^{-1}, which was 1.2 times higher than that in the UV/PMS system. In the UV/H_2O_2-aged MPs system, the k_{obs} of CBZ degradation was 0.70 h^{-1}, which was 1.3 times higher than that in the UV/H_2O_2 system. However, for the UV/Cl-aged MPs system, the k_{obs} of CBZ degradation was 0.36 h^{-1}, which was 1.8 times higher than that in the UV/Cl system. Evidently, the introduction of aged PA MPs significantly increased the k_{obs} of CBZ degradation by 1.2 to 1.8 times across the UV/PMS, UV/H_2O_2, and UV/Cl systems. Notably, although the absolute degradation rate followed the sequence of UV/PMS > UV/H_2O_2 > UV/Cl due to the high quantum yield of PMS and the strong oxidation potential of $SO_4^{\cdot-}$[24], the most pronounced relative enhancement induced by aged MPs was observed in the UV/Cl system. This enhancement clearly underscores that aged MPs do not act merely as inert physical matrices in wastewater. Instead, the EPFRs developed on their surfaces actively participate in electron transfer, thereby specifically driving and accelerating the generation of reactive species in the vicinity of the MPs.

Identification of active species

In this study, electron paramagnetic resonance (EPR) and chemical quenching experiments were used to investigate the main active species involved in the CBZ degradation process in different systems. TBA, FFA, and p-BQ were used as scavengers for ·OH, $^1O_2$, and $O_2^{\cdot-}$[25,26]. In addition, MeOH was selected as a scavenger for ·OH and $SO_4^{\cdot-}$[27], and BA as a scavenger for ·OH and Cl·. As shown in Fig. 2a, b, DMPO-·OH, DMPO-$SO_4^{\cdot-}$, and TEMP-$^1O_2$ signals were detected in the UV/PMS and UV/PMS-aged MPs systems. However, no DMPO-$O_2^{\cdot-}$ signal was detected. The signals of DMPO-·OH and TEMP-$^1O_2$ were more pronounced after the addition of aged MPs, implying that aged MPs mainly increased the production of ·OH and $^1O_2$. As shown in Fig. 2c, when MeOH, TBA, FFA, and p-BQ were added, the k_{obs} values were reduced by 60%, 42%, 39%, and 30%, respectively. This indicated that ·OH, $SO_4^{\cdot-}$, and $^1O_2$ were the main active species in the UV/PMS-aged MPs system. When the oxidant was H_2O_2 (Fig. 2d, e), more ·OH was generated in both UV/H_2O_2 and UV/H_2O_2-aged MPs systems[28].

https://doi.org/10.48130/newcontam-0026-0021

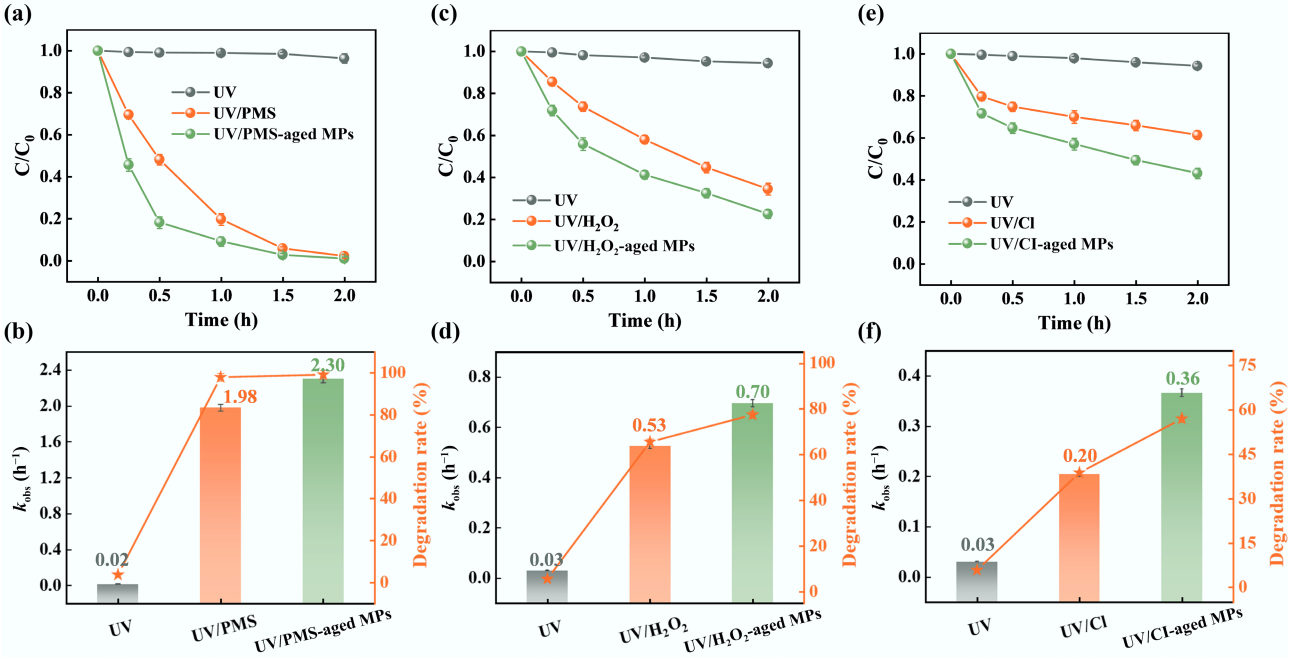

Fig. 1 Effect of aged MPs on CBZ degradation in (**a**), (**b**) UV/PMS, (**c**), (**d**) UV/H_2O_2, and (**e**), (**f**) UV/Cl systems. Reaction conditions: $(CBZ)_0$ = 1 mg·L^{-1}, $(PMS)_0$ = $(H_2O_2)_0$ = $(Cl)_0$ = 0.2 mM, $(PA\ MPs)_0$ = 2 g·L^{-1}, pH = 6.0 ± 0.5, T = 25 °C. k_{obs}, observed pseudo-first-order rate constant. (All experiments were performed in triplicate; error bars are included but are smaller than the symbols in most cases).

Notably, the signals of DMPO-·OH and TEMP-$^1O_2$ were enhanced with the addition of aged MPs, suggesting that more ·OH and $^1O_2$ were produced. With the addition of TBA, k_{obs} was reduced to 0.07 h^{-1}. Similarly, the k_{obs} was reduced by 60% with the addition of FFA (Fig. 2f). Therefore, ·OH and $^1O_2$ played an important role in the degradation of CBZ in the UV/H_2O_2 system. As shown in Fig. 2g, h, a typical DMPOX sevenfold peak was detected in both systems in the presence of NaClO. This was attributed to the ability of DMPO to trap Cl· to form DMPO-Cl· adducts, which in turn were rapidly hydrolyzed to DMPOX derivatives[29]. In addition, signals from TEMP-$^1O_2$ and DMPO-$O_2^{\cdot-}$ were detected. Combining the results of EPR and quenching experiments, it could be concluded that Cl·, ·OH, $^1O_2$, and $O_2^{\cdot-}$ were present in the reaction system, and aged MPs would promote the generation of the above active species. The k_{obs} decreased to 0.22 and 0.19 h^{-1} with the addition of TBA and BA, respectively. This indicated that ·OH and Cl· were the primary active species for CBZ degradation in the UV/Cl system. In all three systems, aged MPs promoted the production of more active species, indicating the importance of aged MPs in CBZ degradation. Previous studies have indicated that environmentally persistent free radicals (EPFRs) generated by MPs can regulate the generation of reactive species, thereby playing significant roles in the aging, biotoxicity, and degradation of MPs. We characterized pristine and aged PA MPs using EPR spectroscopy (Supplementary Fig. S7). Consistent with previous studies on radical generation[30], the aging process induced polymer chain scission and oxidation, leading to the generation of EPFRs on the PA surface, as evidenced by a distinct signal at g = 2.003 (Supplementary Fig. S7). Mechanistically, these aging-induced EPFRs function as highly active electron donors. Under the UV-AOPs conditions, the surface EPFRs facilitate direct single-electron transfer to dissolved oxygen molecules or water, establishing a micro-interfacial catalytic environment that significantly promotes the continuous generation of targeted ROS, particularly ·OH and $^1O_2$[31]. This electron-transfer cascade is a primary driver for the enhanced degradation kinetics. In addition to EPFR-mediated electron transfer, the aging process inherently enriches the surface functional groups and increases the specific surface area of the PA MPs[32,33]. These physicochemical alterations mechanistically contribute to ROS formation by transforming the aged PA into a catalytic substrate. Specifically, the abundant functional groups provide vast active sites for the adsorption of oxidants (i.e., PMS, H_2O_2, and ClO^-). Under UV irradiation, the oxidant molecules concentrated on the MP surface undergo facilitated homolytic cleavage and activation. For instance, in the UV/Cl system, specific oxygen-containing functional groups on the aged MPs could directly react with adsorbed ClO^- to rapidly generate highly reactive chlorine radicals (Cl·)[34]. This critical interfacial mechanism explains the altered radical yields observed in our systems compared to traditional homogeneous UV-AOPs.

Identification of intermediate products and proposed reaction pathways

To further determine the degradation of CBZ in different systems, the degradation intermediates of CBZ were analyzed by UPLC-TOF/MS. As shown in Supplementary Tables S1–S3 and Supplementary Figs. S8–S13, 16 intermediates were identified in the UV/PMS-aged MPs, 14 in the UV/H_2O_2-aged MPs, and 15 in the UV/Cl-aged MPs systems. In addition, we investigated the types and abundance of degradation products of CBZ in different systems (Supplementary Figs. S14–S16). The overall degradation intermediate product content was ranked as follows: UV/PMS system > UV/H_2O_2 system > UV/Cl system. Furthermore, the abundance of CBZ degradation products increased significantly in the presence of aged MPs, especially TPs 228, 167, 226, 284, 151, 149, and 124. Combining the above results, we proposed the degradation pathways of CBZ in different systems. As shown in Fig. 3, a total of 16 degradation intermediates were detected in the system using PMS as the oxidant, based on which we proposed five degradation pathways for CBZ. In the first two pathways, the central heterocycle of CBZ was initially attacked by ·OH and $SO_4^{\cdot-}$, leading to

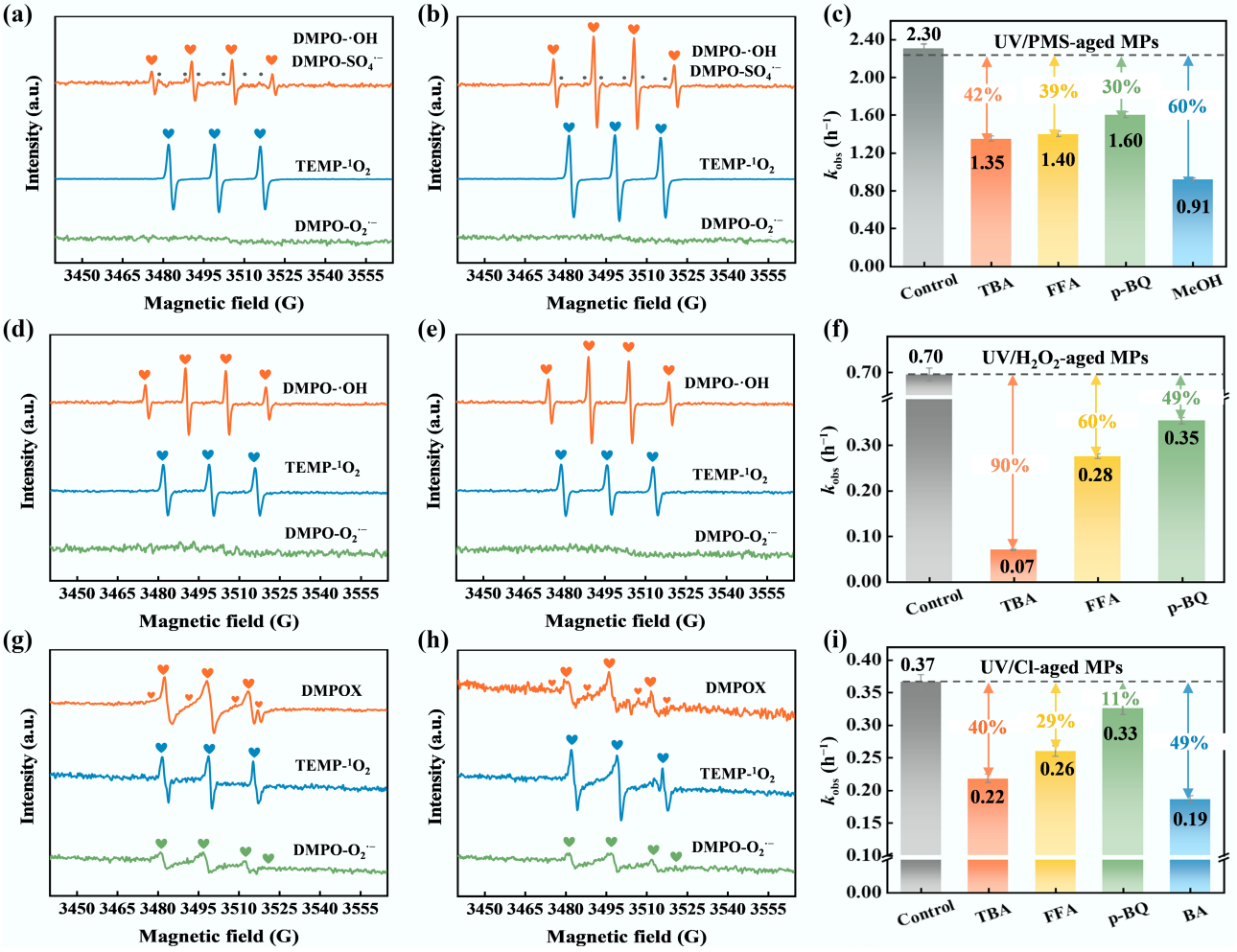

Fig. 2 EPR spectra of active species in the (**a**) UV/PMS, (**b**) UV/PMS-aged MPs, (**d**) UV/H_2O_2, (**e**) UV/H_2O_2-aged MPs, (**g**) UV/Cl, and (**h**) UV/Cl-aged MPs systems. Quenching experiments were conducted in the (**c**) UV/PMS-aged MPs, (**f**) UV/H_2O_2-aged MPs, and (**i**) UV/Cl-aged MPs reaction systems. MeOH, methanol; TBA, tert-butanol; FFA, furfuryl alcohol; p-BQ, *p*-benzoquinone; BA, benzoic acid.

the loss of the –$CONH_2$ group and the formation of TP 194[35]. It was then attacked by ·OH to generate TP 211 and further hydroxylated to form TP 228. Under the attack of ·OH and $SO_4^{\cdot-}$, the central heterocycle of TP 228 broke to produce TP 226. This preferential C–N bond cleavage was attributed to the electron-withdrawing effect of the adjacent carbonyl group, which weakened the neighboring C–N bond, as well as the inherently lower bond dissociation energy of C–N bonds compared with C–C bonds within the heterocycle[36]. Next, TP 226 underwent bond cleavage and oxidation reactions under the attack of ·OH and $^1O_2$[37], decomposing via two pathways. In pathway 1, TP 226 was degraded to TP 149 and TP 124. In pathway 2, TP 226 underwent hydroxylation and oxidation reactions to form TP 167. Under the attack of ·OH, $SO_4^{\cdot-}$, and $^1O_2$, TP 167 generated small molecular compounds TP 151 and TP 116[38]. In the other three pathways, the initiation proceeded via a ring-condensation reaction of CBZ[38], which produced three isomers of TP 253. In pathway 3, TP 253a was attacked by ·OH and $SO_4^{\cdot-}$ to form TP 251[39]. In pathway 4, the carbon atom on the central heterocycle of CBZ was also attacked by $^1O_2$ to form TP 253b[35,40]. TP 253b underwent a ring-condensation reaction under attack by reactive species and lost the –$CONH_2$ group, resulting in the formation of TP 208. TP 208 underwent further bond cleavage, and the carbon atom on the central six-membered ring was oxidized to a carbonyl group to form TP 195[2]. In pathway 5, CBZ could be directly attacked by ·OH to undergo a hydroxylation reaction to produce TP 253c[41]. TP 253c was then hydroxylated to TP 284. Overall, the main reactions involved in the UV/PMS and UV/PMS-aged MPs systems were hydroxylation and ring-condensation reactions. For the UV/H_2O_2 and UV/H_2O_2-aged MPs systems, we also proposed five degradation pathways, as shown in Fig. 4. Similarly, CBZ lost the –$CONH_2$ group to form TP 194 or underwent a ring-condensation reaction to produce three isomers of TP 253. However, compared with the UV/PMS system, there were two differences. First, TP 253b was attacked by ·OH and $^1O_2$, which underwent a ring-condensation and oxidation reaction to directly produce TP 195. Second, TP 167 was attacked by the active species, and the chemical bond was broken to produce the small molecule TP 116. In addition, in the UV/Cl and UV/Cl-aged MPs systems, the presence of Cl· led to the formation of a new compound, TP 241, during the degradation of CBZ (Fig. 5). Notably, TP 241 was generated through TP 284, which lost the –$CONH_2$ group under the attack of ·OH and Cl·[42]. Overall, aged microplastics did not significantly alter the transformation pathway of CBZ within the same system, but different oxidants caused distinct differences in the transformation pathways of CBZ.

By comparing the transformation profiles with and without aged PA, a critical pattern emerged: although the presence of aged PA did not alter the fundamental reaction pathways (i.e., hydroxylation,

https://doi.org/10.48130/newcontam-0026-0021

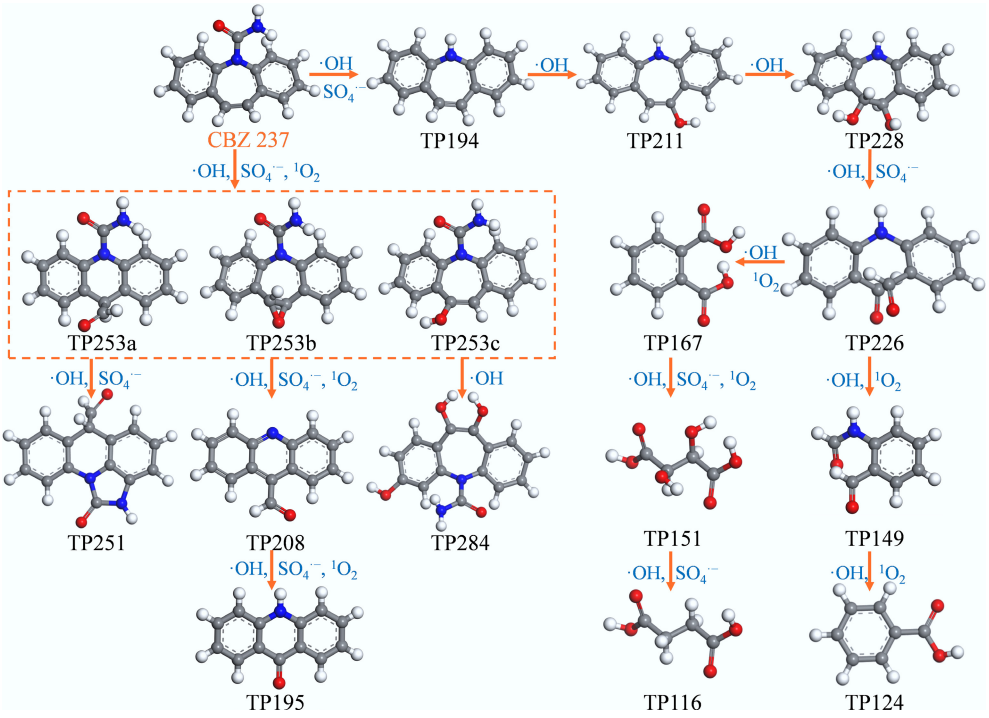

Fig. 3 Degradation pathways of CBZ in UV/PMS and UV/PMS-aged MPs systems.

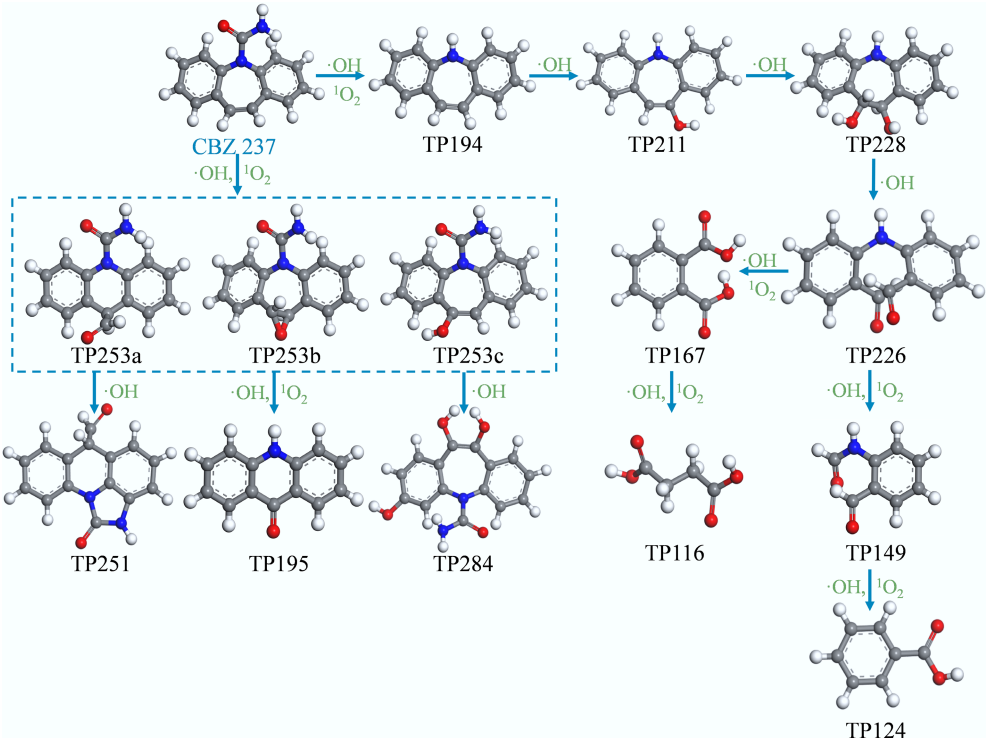

Fig. 4 Degradation pathways of CBZ in UV/H_2O_2 and UV/H_2O_2-aged MPs systems.

ring-condensation, and ring-cleavage) established in conventional AOPs, it profoundly shifted the reaction kinetics and intermediate distribution. As shown in Supplementary Figs. S14–S16, the abundance of specific intermediates (particularly TPs 228, 167, 226, 284, 151, 149, and 124) was substantially increased. This observation provides a crucial mechanistic link: the EPFRs on aged PA surfaces localized the production of ·OH and $^1O_2$ (Fig. 2, Supplementary Fig. S7), which accelerated the electrophilic attack on CBZ and amplified the yield of intermediates. Consequently, since hydroxyl substitution and unsaturated ring formation are closely associated with enhanced toxicity, the presence of aged MPs inevitably shapes the transient toxicity profile of the effluent, highlighting the significant role of aged MPs in the environmental behavior of PPCPs during WWTP processes.

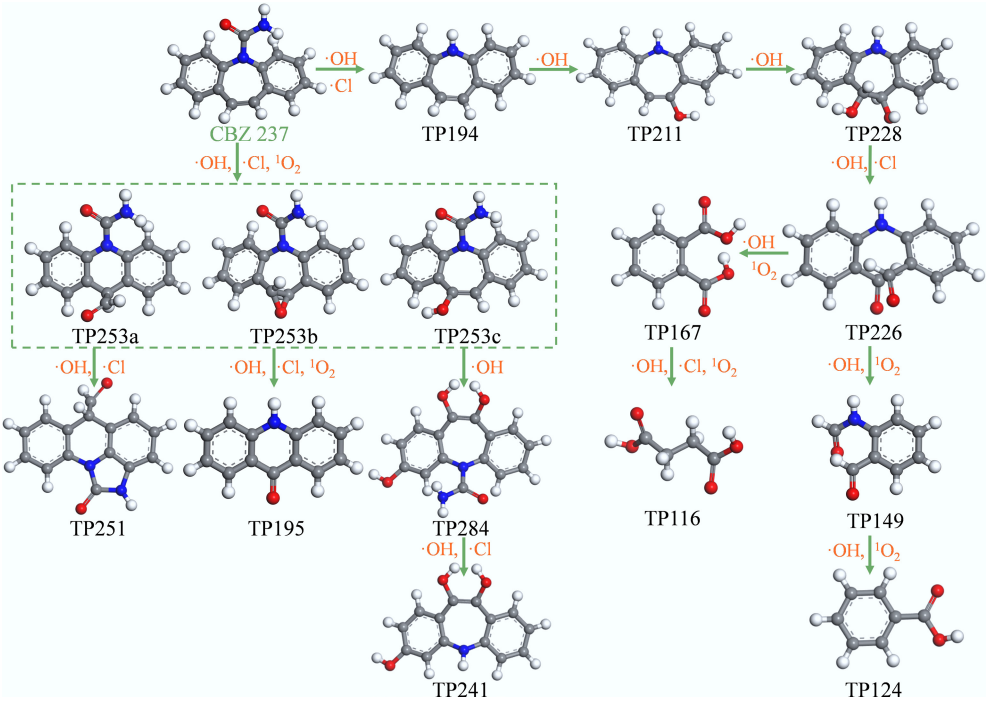

Fig. 5 Degradation pathways of CBZ in UV/Cl and UV/Cl-aged MPs systems.

Toxicity evaluation of degradation intermediates

In this study, the acute and chronic toxicity of CBZ and its intermediates produced in different systems to aquatic organisms (e.g., fish, daphnia, and green algae) was evaluated by ECOSAR, as shown in Supplementary Table S4 and Fig. 6. The acute and chronic toxicity of TP 194 was much higher than that of CBZ, especially for daphnia. In addition, TPs 211, 226, and 208 showed higher acute and chronic toxicity to fish, daphnia, and green algae than CBZ, and were categorized as 'harmful' and 'toxic'. These results suggested that the process of degradation and transformation of organic pollutants might produce products that were more toxic than their parent compounds. Analysis of the toxicity and molecular structures of the intermediates revealed that the increased toxicity of the intermediates was attributed to the removal of the $-CONH_2$ group from the central heterocycle of CBZ, hydroxyl substitution reactions, and the formation of unsaturated six-membered rings[43,44]. Furthermore, for these three intermediates, the concentrations in the UV/PMS-aged MPs, UV/H_2O_2-aged MPs, and UV/Cl-aged MPs systems were slightly higher than those in the UV/PMS, UV/H_2O_2, and UV/Cl systems (Supplementary Figs. S14–S16). Additionally, the toxicity of other intermediates was much lower than that of CBZ. In the presence of aged MPs, the total toxicity of intermediates produced by CBZ degradation in different reaction systems depended on the composition of the intermediates, and the abundances of the intermediates also played a crucial role. Given the elevated toxicity of these MP-mediated intermediates, implementing upstream microplastic removal (e.g., coagulation or filtration) prior to AOP units is highly recommended as a practical engineering strategy to prevent the formation of highly toxic effluents. Although small amounts of toxic intermediates were generated in this study, they could eventually be degraded to low-molecular-weight and less toxic substances (e.g., TPs 151 and 116) as the degradation reaction proceeded. Notably, aged PA did not alter the inherent toxicity trend of the intermediates but moderately increased their absolute abundances, and these transient toxic intermediates could be further degraded to non-toxic products with extended reaction time.

Impact and correlation analysis of environmental factors

Inorganic ions and dissolved organic matter in wastewater may affect the degradation and transformation of CBZ. Therefore, the effects of various influencing factors on CBZ degradation, including anions (NO_3^-, Cl^-, HCO_3^-), typical dissolved organic matter (humic acid), and pH, were systematically investigated. As shown in Supplementary Fig. S17, for the UV/PMS-aged MPs system, the k_{obs} for CBZ in the presence of NO_3^- increased to 2.71 h^{-1} as the concentration increased to 10 mM. This can be attributed to the fact that NO_3^- would participate in the free radical reaction, promoting the degradation of CBZ by generating more ·OH as well as reactive nitrogen species ($\cdot NO_2$, ·NO, $ONOO^-$) in the reaction schemes as in Eqs. (1) to (3)[45]. When Cl^- was present, the k_{obs} for CBZ degradation increased to 2.62 h^{-1}, implying that Cl^- promoted the degradation of CBZ. This was due to the formation of chlorine-containing radicals (Cl·, $Cl_2^{\cdot-}$, Cl_2, HClO, and ClO·) as shown in Eqs. (4) to (12)[46]. In addition, PMS and Cl^- could react directly to form HClO. HCO_3^- inhibited the rate of CBZ degradation, and the k_{obs} decreased from 2.30 to 1.81 h^{-1}, which can be attributed to the fact that HCO_3^- reacted with ·OH and $SO_4^{\cdot-}$ to generate radicals with lower oxidizing capacity, as shown in Eqs. (13) and (14)[47]. As shown in Supplementary Fig. S18, humic acid reduced the degradation k_{obs} of CBZ to 1.42 h^{-1}. Humic acid can not only absorb photons, but also react with active species, thus reducing the rate of CBZ degradation[48]. Furthermore, the effect of pH on the degradation of CBZ in the UV/PMS-aged MPs system was not significant, and the degradation of CBZ was slightly enhanced under acidic conditions.

In the UV/H_2O_2-aged MPs system, as shown in Supplementary Fig. S19, the k_{obs} of CBZ degradation increased from 0.70 to 2.12 h^{-1} as the NO_3^- concentration increased from 0 to 10 mM. This could be attributed to the ability of NO_3^- to produce reactive species (e.g., ·OH) under light irradiation[49]. Cl^- significantly promoted the degradation of CBZ by the UV/H_2O_2-aged MPs system, increasing the k_{obs} to 2.32 h^{-1}. The possible reactions in the reaction system are shown

https://doi.org/10.48130/newcontam-0026-0021

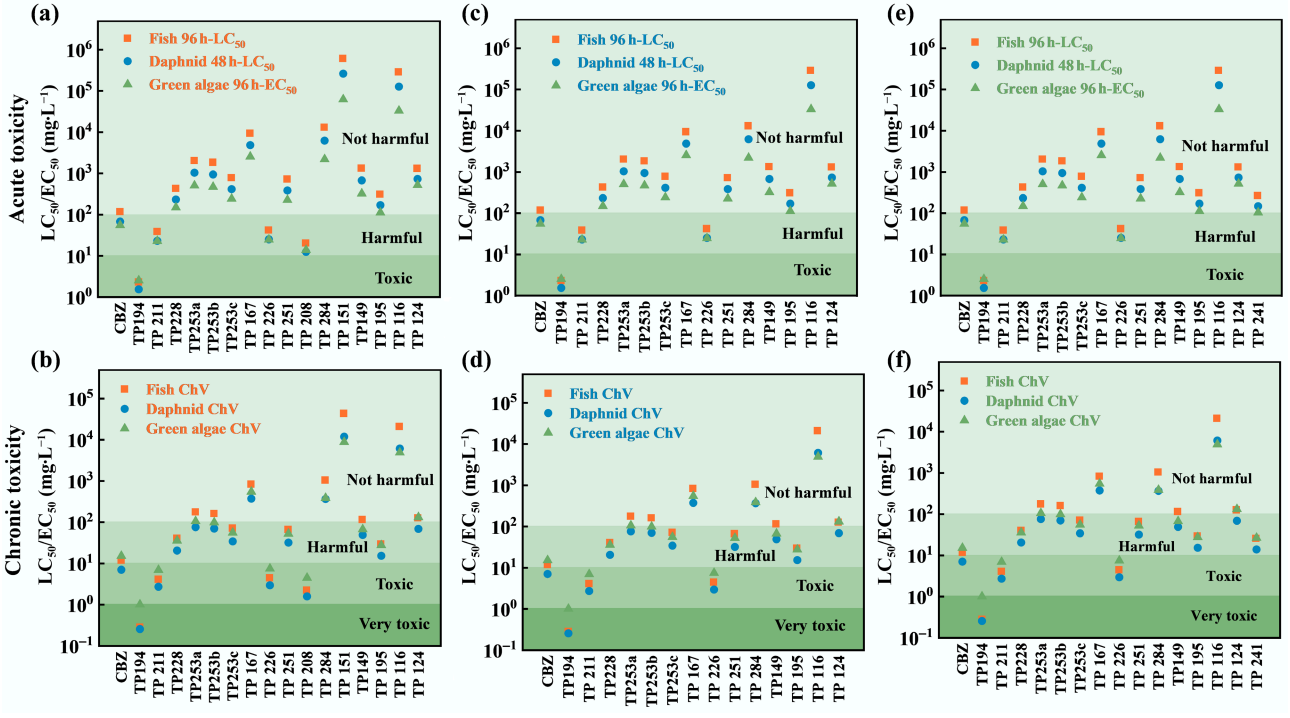

Fig. 6 Toxicity of CBZ and its degradation intermediates obtained by the ECOSAR program (**a**), (**b**) UV/PMS system, (**c**), (**d**) UV/H_2O_2 system, and (**e**), (**f**) UV/Cl system. The intermediate labels correspond to the transformation products identified in the degradation pathways shown in Figs. 3–5.

in Eqs. (4) to (12). As shown in Supplementary Fig. S19e, S19f, HCO_3^- slightly inhibited the degradation rate of CBZ, reducing k_{obs} from 0.70 to 0.67 h^{-1} (Eq. [13]). Humic acid also inhibited the rate of CBZ degradation (Supplementary Fig. S20). Unlike the UV/PMS-aged MPs system, the k_{obs} of CBZ degradation in the UV/H_2O_2-aged MPs system was 2.3 times higher in acidic conditions than in neutral conditions. This pH-dependent behavior can be attributed to several factors. First, the speciation of CBZ varies with pH; the protonated form of CBZ under acidic conditions exhibits higher reactivity toward ·OH attack compared with its neutral form at neutral pH. Second, increased OH^- concentration at higher pH scavenges ·OH via ·OH + $OH^- \rightarrow H_2O + O^{\cdot-}$, reducing the steady-state concentration of ·OH available for CBZ degradation. Third, the quantum yield of H_2O_2 photolysis and the subsequent ·OH generation efficiency are also pH-dependent. These combined effects result in higher degradation rates under acidic conditions compared with neutral pH in the UV/H_2O_2 system[50].

For the UV/Cl-aged MPs system, k_{obs} increased from 0.37 to 1.68 h^{-1} with increasing NO_3^- concentration (Eqs. [1] to [3]), as shown in Supplementary Fig. S21. In contrast to the above two systems, Cl^- would not significantly affect the degradation of CBZ in the UV/Cl-aged MPs system (Supplementary Fig. S21d). This was due to the ability of Cl^- to promote the production of strongly oxidizing species to enhance the rate of degradation reactions[51]. As shown in Supplementary Fig. S21f, HCO_3^- reacted with ·OH and Cl· to form less reactive $CO_3^{\cdot-}$, H_2O, and HCl (as shown in Eqs. [13] and [14]), thereby reducing the k_{obs} to 0.10 h^{-1}[52]. Similarly, humic acid significantly inhibits the degradation of CBZ (Supplementary Fig. S22). This is because humic acid contains a variety of functional groups such as hydroxyl, carbonyl, and phenol groups, which can competitively consume ·OH and Cl· in the reaction system[53]. Additionally, acidic conditions had little effect on CBZ degradation, whereas alkaline conditions markedly inhibited CBZ degradation.

Based on the above analysis, various environmental factors could participate in the radical reaction, which subsequently affected the degradation of organic pollutants in different systems. We summarized the effects of environmental factors on CBZ degradation in different systems by Pearson correlation analysis using anions (NO_3^-, Cl^-, and HCO_3^-) as well as k_{obs} from humic acid experiments as shown in Fig. 7. In the UV/PMS-aged MPs and UV/H_2O_2-aged MPs systems, NO_3^- and Cl^- concentrations were positively correlated with the k_{obs} of CBZ degradation (* $p \leq 0.05$), whereas HCO_3^- and humic acid concentrations were negatively correlated with the k_{obs} of CBZ degradation (* $p \leq 0.05$). In contrast, in the UV/Cl-aged MPs system, only NO_3^- concentration was positively correlated with CBZ degradation k_{obs}, whereas Cl^-, HCO_3^-, and humic acid concentrations were negatively correlated with CBZ degradation k_{obs}. In summary, NO_3^- promoted CBZ degradation in all the above UV-AOP systems. The effect of Cl^- on the degradation reaction depended on the concentration of Cl^- and the type of reaction system, and both HCO_3^- and humic acid inhibited CBZ degradation. Various anions and dissolved organic matter would affect the degradation of CBZ in the system, and the effect of environmental factors on the degradation of pollutants depended on their participation in the process of free radical generation and transformation[54,55].

$$NO_3^- + h\nu \rightarrow \cdot NO_2 + O^{\cdot-} (O^{\cdot-} + H_2O \rightleftharpoons \cdot OH + OH^-) \quad (1)$$

$$NO_3^- + H^+ + h\nu \rightarrow ONOO^- + H^+ \rightleftharpoons ONOOH \quad (2)$$

$$ONOOH \rightleftharpoons \cdot NO_2 + \cdot OH \quad (3)$$

$$\cdot OH + Cl^- \rightarrow ClOH^{\cdot-} \quad (4)$$

$$ClOH^{\cdot-} + H^+ \rightarrow Cl\cdot + H_2O \quad (5)$$

$$Cl\cdot + Cl^- \rightarrow Cl_2^{\cdot-} \quad (6)$$

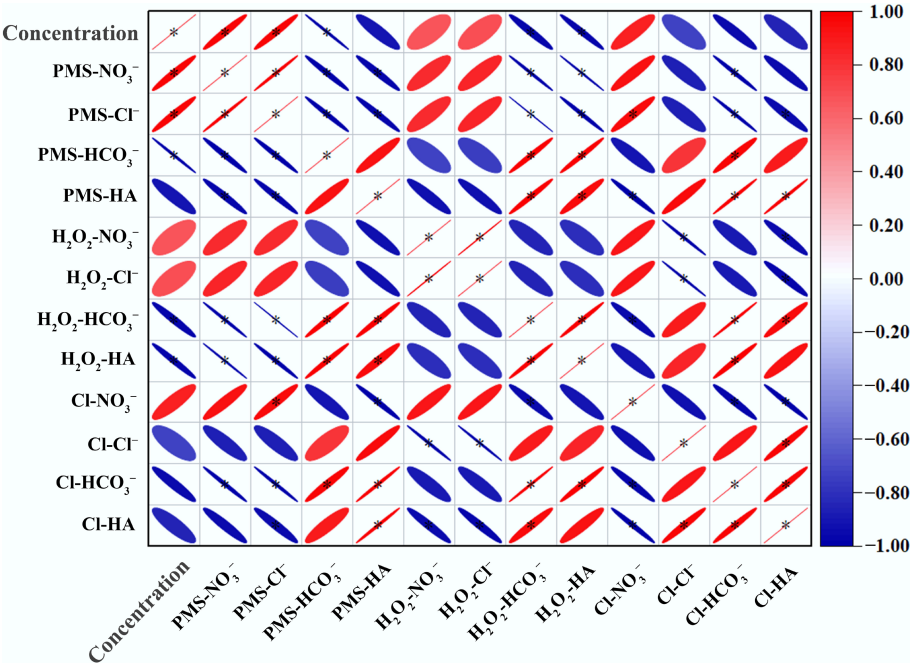

Fig. 7 Pearson correlation analysis of the effect of different concentrations of anions and humic acid (HA) on CBZ degradation. The red and blue colors indicate positive and negative correlations, respectively, and the depth of the color indicates the strength of the correlation. * $p \leq 0.05$ indicates a statistically significant correlation.

$$Cl\cdot + Cl_2^{\cdot-} \rightarrow Cl_2 + Cl^- \quad (7)$$

$$Cl_2^{\cdot-} + Cl_2^{\cdot-} \rightarrow Cl_2 + 2Cl^- \quad (8)$$

$$HSO_5^- + Cl^- \rightarrow SO_4^{2-} + HClO \quad (9)$$

$$Cl_2 + H_2O \rightleftharpoons H^+Cl^- + HClO \quad (10)$$

$$HClO + \cdot OH \rightarrow ClO\cdot + H_2O \quad (11)$$

$$Cl\cdot/Cl_2^{\cdot-}/ClO\cdot/HClO + CBZ \rightarrow \text{Products} \quad (12)$$

$$HCO_3^- + \cdot OH \rightarrow H_2O + CO_3^{\cdot-} \quad (13)$$

$$HCO_3^- + SO_4^{\cdot-} \rightarrow HSO_4^- + CO_3^{\cdot-} \quad (14)$$

Conclusions

Herein, the interfacial mechanism between aged MPs and CBZ in UV/PMS, UV/H_2O_2, and UV/Cl systems, and the effect of aged PA MPs on the degradation properties of CBZ in different UV-AOPs were investigated. The degradation rates and k_{obs} of CBZ in different UV-AOPs followed the sequence: UV/PMS > UV/H_2O_2 > UV/Cl > UV. Combined with EPR and chemical quenching experiments, it was found that ·OH, $SO_4^{\cdot-}$, and $^1O_2$ played important roles in the degradation of CBZ in the UV/PMS system; ·OH and $^1O_2$ were the main reactive oxygen species for the degradation of CBZ in the UV/H_2O_2 system; and Cl·, ·OH, and $^1O_2$ contributed to the degradation of CBZ in the UV/Cl system to different degrees. In addition, aged MPs mainly increased the production of ·OH and $^1O_2$. We proposed degradation pathways for CBZ in different systems involving hydroxylation, oxidation, and ring cleavage reactions. The differences in degradation pathways in different UV-AOPs were mainly in TPs 208, 151, and 241. The toxicity and molecular structure analyses of the intermediates revealed that most of the CBZ degradation intermediates were less toxic than CBZ. The total toxicity of CBZ degradation intermediates in the presence of aged MPs depended on the composition and content of the products. Furthermore, various anions (NO_3^-, Cl^-, and HCO_3^-) and dissolved organic matter (humic acid) could all influence the degradation of CBZ in the system. The role of environmental factors in pollutant degradation was attributed to the fact that they would participate in free radical generation and transformation processes. This study provides a theoretical basis for elucidating the environmental behaviors of MPs and PPCPs during the treatment of wastewater in WWTPs. As only PA was tested, future studies will systematically compare a wider range of MP types. Nevertheless, the present study was conducted under controlled laboratory conditions, and the behavior of aged MPs and associated EPFRs in complex natural waters requires further verification. Future studies should evaluate these effects under environmentally relevant conditions and further assess the fate, toxicity, and ecological risks of the resulting transformation products.

Ethical statements

This work does not involve any human or animal studies. All experiments were performed with non-biological materials, and thus formal ethical approval was not required.

Author contributions

The authors confirm their contributions to the paper as follows: Yuhui Wang, Xiaohui Wang, Tingting Zhang: study conception and design; Yuhui Wang, Xiaochao Zhou: analysis and interpretation of results; Yuhui Wang, Xiaochao Zhou, Hang Liu: draft manuscript preparation; Yuhui Wang, Xiaochao Zhou, Zhenyang Xu, Hang Liu: data collection; All authors reviewed the results and approved the final version of the manuscript.

Data availability

The datasets generated during and/or analyzed during the current study are available from the corresponding author upon reasonable request.

Acknowledgments

No acknowledgements are applicable for this work.

Funding

This work was financially supported by the National Natural Science Foundation of China (Grant No. 41977142).

Declarations

Conflict of interest

The authors declare that they have no known competing financial interests or personal relationships that could have appeared to influence the work reported in this paper.

Author details

Department of Environmental Science and Engineering, College of Chemical Engineering, Beijing University of Chemical Technology, Beijing 100029, China

References

[1] Cui Y, Wang Y, Pan C, Li R, Xue R, et al. 2019. Spatiotemporal distributions, source apportionment and potential risks of 15 pharmaceuticals and personal care products (PPCPs) in Qinzhou Bay, South China. *Marine Pollution Bulletin* 141:104−111

[2] Cao J, Nie W, Huang L, Ding Y, Lv K, et al. 2019. Photocatalytic activation of sulfite by nitrogen vacancy modified graphitic carbon nitride for efficient degradation of carbamazepine. *Applied Catalysis B: Environmental* 241:18−27

[3] Chen G, Dong W, Wang H, Zhao Z, Wang F, et al. 2022. Carbamazepine degradation by visible-light-driven photocatalyst Ag_3PO_4/GO: mechanism and pathway. *Environmental Science and Ecotechnology* 9:100143

[4] Hu J, Lim FY, Hu J. 2023. Characteristics and behaviors of microplastics undergoing photoaging and Advanced Oxidation Processes (AOPs) initiated aging. *Water Research* 232:119628

[5] Zhou G, Wu Q, Wei XF, Chen C, Ma J, et al. 2023. Tracing microplastics in rural drinking water in Chongqing, China: their presence and pathways from source to tap. *Journal of Hazardous Materials* 459:132206

[6] Pivokonsky M, Cermakova L, Novotna K, Peer P, Cajthaml T, et al. 2018. Occurrence of microplastics in raw and treated drinking water. *Science of the Total Environment* 643:1644−1651

[7] Zhao S, Xue S, Zhang J, Zhang Z, Sun J. 2020. Dissolved organic matter-mediated photodegradation of anthracene and pyrene in water. *Scientific Reports* 10:3413

[8] Yang Z, Liu P, Wang J, Ding L, Li L, et al. 2023. Microplastics-derived dissolved organic matters accelerate photodegradation of sulfamethazine in wastewater ultraviolet disinfection process. *Chemical Engineering Journal* 454:140301

[9] Sun J, Dai X, Wang Q, van Loosdrecht MCM, Ni BJ. 2019. Microplastics in wastewater treatment plants: detection, occurrence and removal. *Water Research* 152:21−37

[10] Zou W, Xia M, Jiang K, Cao Z, Zhang X, et al. 2020. Photo-oxidative degradation mitigated the developmental toxicity of polyamide microplastics to zebrafish larvae by modulating macrophage-triggered proinflammatory responses and apoptosis. *Environmental Science & Technology* 54:13888−13898

[11] Tong X, Mohapatra S, Zhang J, Tran NH, You L, et al. 2022. Source, fate, transport and modelling of selected emerging contaminants in the aquatic environment: current status and future perspectives. *Water Research* 217:118418

[12] Hu CY, Hu LL, Dong ZY, Yang XY, Liu H, et al. 2024. Enhanced degradation of emerging contaminants by Far-UVC photolysis of peracetic acid: synergistic effect and mechanisms. *Water Research* 260:121943

[13] Ao X, Liu W, Sun W, Yang C, Lu Z, et al. 2018. Mechanisms and toxicity evaluation of the degradation of sulfamethoxazole by MPUV/PMS process. *Chemosphere* 212:365−375

[14] Chaves FP, Gomes G, Della-Flora A, Dallegrave A, Sirtori C, et al. 2020. Comparative endocrine disrupting compound removal from real wastewater by UV/Cl and UV/H_2O_2: effect of pH, estrogenic activity, transformation products and toxicity. *Science of the Total Environment* 746:141041

[15] Cheng S, Zhang X, Yang X, Shang C, Song W, et al. 2018. The multiple role of bromide ion in PPCPs degradation under UV/chlorine treatment. *Environmental Science & Technology* 52:1806−1816

[16] Sun Y, Peng M, Zhang Q, Zhang X, Xu X, et al. 2025. Aging of microplastics and its photo-catalytic degradation of coexisting tetracycline. *Separation and Purification Technology* 355:129605

[17] Wang H, Liu P, Wang M, Wu X, Shi Y, et al. 2021. Enhanced phototransformation of atorvastatin by polystyrene microplastics: critical role of aging. *Journal of Hazardous Materials* 408:124756

[18] Wang J, Zhang J, Guo K, Yue Q, Li Y, et al. 2024. Selective elimination of organic pollutants and analysis of effects and novel mechanisms of aged microplastics on wavelength-dependent UV-LED/H_2O_2 system. *Water Research* 267:122526

[19] Wang Y, Zhao W, Pang Y, Fu S, Xu Z, et al. 2025. In-situ growth of Fe clusters on MXene for fluorinated fire-fighting foam wastewater purification in peroxone system. *Chemical Engineering Journal* 508:160883

[20] Wang J, Liu S, Chen S, Long Y, Lou Y, et al. 2025. Insights into the photoaging behavior of microplastics: environmental fate and ecological risk. *Environmental Science & Technology* 59:23673−23690

[21] Guo R, Qi Y, Li B, Tian J, Wang Z, et al. 2022. Efficient degradation of alkyl imidazole ionic liquids in simulated sunlight irradiated periodate system: kinetics, reaction mechanisms, and toxicity evolution. *Water Research* 226:119316

[22] Metz J, Zuo P, Wang B, Wong MS, Alvarez PJJ. 2022. Perfluorooctanoic acid degradation by UV/chlorine. *Environmental Science & Technology Letters* 9:673−679

[23] Yang B, Wang C, Cheng X, Zhang Y, Li W, et al. 2021. Interactions between the antibiotic tetracycline and humic acid: examination of the binding sites, and effects of complexation on the oxidation of tetracycline. *Water Research* 202:117379

[24] Yang J, Xie T, Mei Y, Chen J, Sun H, et al. 2023. High-efficiency V-Mediated Bi_2MoO_6 photocatalyst for PMS activation: modulation of energy band structure and enhancement of surface reaction. *Applied Catalysis B: Environmental* 339:123149

[25] Ji H, Du P, Zhao D, Li S, Sun F, et al. 2020. 2D/1D graphitic carbon nitride/titanate nanotubes heterostructure for efficient photocatalysis of sulfamethazine under solar light: catalytic "hot spots" at the rutile–anatase–titanate interfaces. *Applied Catalysis B: Environmental* 263:118357

[26] Gao L, Guo Y, Zhan J, Yu G, Wang Y. 2022. Assessment of the validity of the quenching method for evaluating the role of reactive species in pollutant abatement during the persulfate-based process. *Water Research* 221:118730

[27] Yao J, Wu N, Tang X, Wang Z, Qu R, et al. 2022. Methyl phenyl sulfoxide (PMSO) as a quenching agent for high-valent metal-oxo species in peroxymonosulfate based processes should be reconsidered. *Chemical Engineering Journal Advances* 12:100378

[28] Kim MS, Lee C, Kim JH. 2021. Occurrence of unknown reactive species in UV/H_2O_2 system leading to false interpretation of hydroxyl radical probe reactions. *Water Research* 201:117338

[29] Huang X, Wang Y, Li X, Guan D, Li Y, et al. 2019. Autocatalytic decomplexation of Cu(II)–EDTA and simultaneous removal of aqueous Cu(II) by UV/chlorine. *Environmental Science & Technology* 53:2036–2044
[30] Zhu K, Jia H, Zhao S, Xia T, Guo X, et al. 2019. Formation of environmentally persistent free radicals on microplastics under light irradiation. *Environmental Science & Technology* 53:8177–8186
[31] Liu S, Huang W, Yang J, Xiong Y, Huang Z, et al. 2023. Formation of environmentally persistent free radicals on microplastics under UV irradiations. *Journal of Hazardous Materials* 453:131277
[32] Ding R, Ouyang Z, Bai L, Zuo X, Xiao C, et al. 2022. What are the drivers of tetracycline photolysis induced by polystyrene microplastic? *Chemical Engineering Journal* 435:134827
[33] Jiang L, Xie S, Chen H, Yang J, Wang X, et al. 2025. Visible-light-promoted peroxymonosulfate activation for ACE degradation: overlooked role of photogenerated hole. *Applied Catalysis B: Environment and Energy* 365:124881
[34] Liu X, Sun P, Qu G, Jing J, Zhang T, et al. 2021. Insight into the characteristics and sorption behaviors of aged polystyrene microplastics through three type of accelerated oxidation processes. *Journal of Hazardous Materials* 407:124836
[35] Trognon J, Albasi C, Choubert JM. 2024. A critical review on the pathways of carbamazepine transformation products in oxidative wastewater treatment processes. *Science of the Total Environment* 912:169040
[36] Deng J, Ye C, Cai A, Huai L, Zhou S, et al. 2021. S-doping α-Fe_2O_3 induced efficient electron-hole separation for enhanced persulfate activation toward carbamazepine oxidation: experimental and DFT study. *Chemical Engineering Journal* 420:129863
[37] Meng Y, Li Z, Tan J, Li J, Wu J, et al. 2022. Oxygen-doped porous graphitic carbon nitride in photocatalytic peroxymonosulfate activation for enhanced carbamazepine removal: performance, influence factors and mechanisms. *Chemical Engineering Journal* 429:130860
[38] Roy K, Moholkar VS. 2021. Mechanistic analysis of carbamazepine degradation in hybrid advanced oxidation process of hydrodynamic cavitation/UV/persulfate in the presence of ZnO/$ZnFe_2O_4$. *Separation and Purification Technology* 270:118764
[39] Wang X, Ao X, Zhang T, Li Z, Cai R, et al. 2022. Ultraviolet-Light-emitting-diode activated monochloramine for the degradation of carbamazepine: kinetics, mechanisms, by-product formation, and toxicity. *Science of the Total Environment* 806:151372
[40] Bu L, Zhou S, Zhu S, Wu Y, Duan X, et al. 2018. Insight into carbamazepine degradation by UV/monochloramine: reaction mechanism, oxidation products, and DBPs formation. *Water Research* 146:288–297
[41] Wang WL, Wu QY, Huang N, Wang T, Hu HY. 2016. Synergistic effect between UV and chlorine (UV/chlorine) on the degradation of carbamazepine: influence factors and radical species. *Water Research* 98:190–198
[42] Qin W, Liu Z, Lin Z, Wang Y, Dong H, et al. 2022. Unraveling the multiple roles of VUV mediated hydroxyl radical in VUV/UV/chlorine process: kinetic simulation, mechanistic consideration and byproducts formation. *Chemical Engineering Journal* 446:137066
[43] Wang Y, Yan P, Dou X, Liu C, Zhang Y, et al. 2021. Degradation of benzophenone-4 by peroxymonosulfate activated with microwave synthesized well-distributed $CuBi_2O_4$ microspheres: theoretical calculation of degradation mechanism. *Applied Catalysis B: Environmental* 290:120048
[44] Cui T, Xiao Z, Wang Z, Liu C, Song Z, et al. 2021. FeS_2/carbon felt as an efficient electro-Fenton cathode for carbamazepine degradation and detoxification: in-depth discussion of reaction contribution and empirical kinetic model. *Environmental Pollution* 282:117023
[45] Wang S, Luo C, Tan F, Cheng X, Ma Q, et al. 2021. Degradation of Congo red by UV photolysis of nitrate: kinetics and degradation mechanism. *Separation and Purification Technology* 262:118276
[46] Huang Y, Sheng B, Wang Z, Liu Q, Yuan R, et al. 2018. Deciphering the degradation/chlorination mechanisms of maleic acid in the Fe(II)/peroxymonosulfate process: an often overlooked effect of chloride. *Water Research* 145:453–463
[47] Fang Y, Devon J, Rao D, Liu J, Schaefer C. 2024. Destruction of perfluorooctane sulfonic acid (PFOS) in gas sparging incorporated UV-indole reductive treatment system – benefits and challenges. *Journal of Hazardous Materials* 480:135935
[48] Tu Z, Qi Y, Qu R, Tang X, Wang Z, et al. 2022. Photochemical transformation of hexachlorobenzene (HCB) in solid-water system: kinetics, mechanism and toxicity evaluation. *Chemosphere* 295:133907
[49] Ding X, Gutierrez L, Croue JP, Li M, Wang L, et al. 2020. Hydroxyl and sulfate radical-based oxidation of RhB dye in UV/H_2O_2 and UV/persulfate systems: kinetics, mechanisms, and comparison. *Chemosphere* 253:126655
[50] Ye C, Ma X, Deng J, Li X, Li Q, et al. 2022. Degradation of saccharin by UV/H_2O_2 and UV/PS processes: a comparative study. *Chemosphere* 288:132337
[51] Zhu KA, Chen XJ, Yuan CW, Bai CW, Sun YJ, et al. 2023. Orientated construction of visible-light-assisted peroxymonosulfate activation system for antibiotic removal: significant enhancing effect of Cl^-. *Journal of Hazardous Materials* 445:130476
[52] Wu N, Xiang W, Zhu F, Huo Z, Wang Z, et al. 2023. Oxidative degradation and possible interactions of coexisting decabromodiphenyl ether (BDE-209) on polystyrene microplastics in UV/chlorine process. *Water Research* 245:120560
[53] Fang J, Fu Y, Shang C. 2014. The roles of reactive species in micropollutant degradation in the UV/free chlorine system. *Environmental Science & Technology* 48:1859–1868
[54] Chen C, Chen L, Yao Y, Artigas F, Huang Q, et al. 2019. Organotin release from polyvinyl chloride microplastics and concurrent photodegradation in water: impacts from salinity, dissolved organic matter, and light exposure. *Environmental Science & Technology* 53:10741–10752
[55] Guo K, Wu Z, Yan S, Yao B, Song W, et al. 2018. Comparison of the UV/chlorine and UV/H_2O_2 processes in the degradation of PPCPs in simulated drinking water and wastewater: kinetics, radical mechanism and energy requirements. *Water Research* 147:184–194